Responses to the comments of Reviewer 2

We, the authors, would like to extend our sincere gratitude to the reviewer for their valuable time and efforts invested in reading the manuscript. We appreciate and acknowledge all the comments, feedback, and constructive suggestions provided for the further improvement of the manuscript by the reviewer. We have tried to respond to each of the comments with the best possible clarifications, while considering the feedback, and have attempted to carefully incorporate the suggestions given by the reviewer. The responses to each of the specific comments and the corresponding figures for the clarifications are compiled below.

1. *The authors use global gravity data and upward continue Bouguer gravity anomaly to investigate the crustal structure within the study area. I understand that upward continuing acts as a low pass filter to enhance the long-wavelength regional Bouguer anomaly trend.*

   Please, can the authors explain why they chose 30 km elevation for the upward continuation? Is 30 km the elevation at which the effect of surface structures become negligible?

   It would be interesting to provide a few test examples of upward continuation at different elevations (possibly as supplementary material); also, see e.g. Zeng et al. (2007), Geophysics, for approaches to estimate ideal elevation for upward continuation.

   Also, the terrain correction seems to be small (less than 1 mGal), but topography ranges from 175 m to 617 m (line 152). Can the authors provide a topographic map of the study area, together with the grid points from the global gravity data they used?

   Response: We would like to clarify that the choice of the upward continuing heights was based on a trial-and-error approach as suggested by Gupta and Ramani (1980). The 30 km upward continued regional gravity anomaly shows some similarities with the overall trend observed in the complete Bouguer anomaly map (Fig. 1, below). Consequently, the corresponding residual gravity anomaly obtained after removing the 30 km upward continued regional gravity anomaly also showed some correlations with the lithological units observed in Figure 1b of the manuscript. Thus, these maps were the ones included in the manuscript and utilized these results to understand the high-density sources causing these signatures at various depths.

   We thank the reviewer for the suggestion based on the work of Zeng et al. (2007) where they demonstrated a logical procedure for selection of best upward continued height for regional-residual separation. However, they concluded that their method also gave

ambiguous choice of upward continued heights for separation of gravity anomaly due to multiple sources and there is no optimum height. Based on the theoretical concept, several authors also consider the upward continuation height as twice the value of the source depth (Jacobsen, 1987; Meng et al., 2009; Pal and Kumar, 2019; Kebede et al., 2020). Thus, following the suggestions provided, we have now added the regional-residual gravity anomaly results based on the upward continuation heights of 60 km, 30 km, and 10 km (Figs. 2A, 2B, 2C, respectively, see below) approximately corresponding to the depth estimates from radially averaged power spectrum analysis, i.e., ~30.3 km, ~11.9 km, and ~2.7 km, respectively. The 60 km ed upward continued regional gravity anomaly show the moderate to high anomalies trending from the central region up to the SW corner of the study area. The regional and residual gravity anomaly maps obtained by the 10 km upward continuation method (Fig. 2C) show similarity to those obtained from the 30 km upward continuation method (Fig. 2B). These show the signatures from the high-density sources from deeper as well as shallower depths. Therefore, based on the above observations and the geological setup of this region, we infer that the magmatic emplacement as an underplated layer at the lower crustal levels as well as the volcanogenic rock sequences of the Bijawar group at shallower depth (Mishra, 2015) may have caused such anomaly patterns in the upward continued regional gravity anomaly maps and the corresponding residual gravity anomaly maps.

We thank the reviewer for their suggestion here related to the terrain correction and the required modifications are incorporated in the revised manuscript. The topography map for the study area is presented here in the Figure 3a, showing a variation from175 m to 617 m, derived from the global 1-minute topography grids available on the website of the Scripps Institution of Oceanography (Smith and Sandwell, 1997). The terrain correction is calculated and applied using the Terrain module available on the Geosoft Oasis Montaj software, and on cross-checking with the values derived from the module, the maximum terrain correction obtained is ~ 0.93 mGal. We sincerely apologise for overlooking this. This has now been rectified in the revised manuscript. A plot depicting the terrain correction values calculated over the study area is presented in the Figure 3b. The Bouguer anomaly map without terrain correction (Fig. 4a) and the complete Bouguer anomaly map (Fig. 4b) after the application of the terrain correction is observed to be of similar in trend. Since the plotted topographic map is derived from a global 1-minute gridded data, plotting the gravity data points on the topographic map results in a map with densely populated grid points,

obscuring the observed topographic variations. Thus, we have avoided plotting the data points on the topographic map.

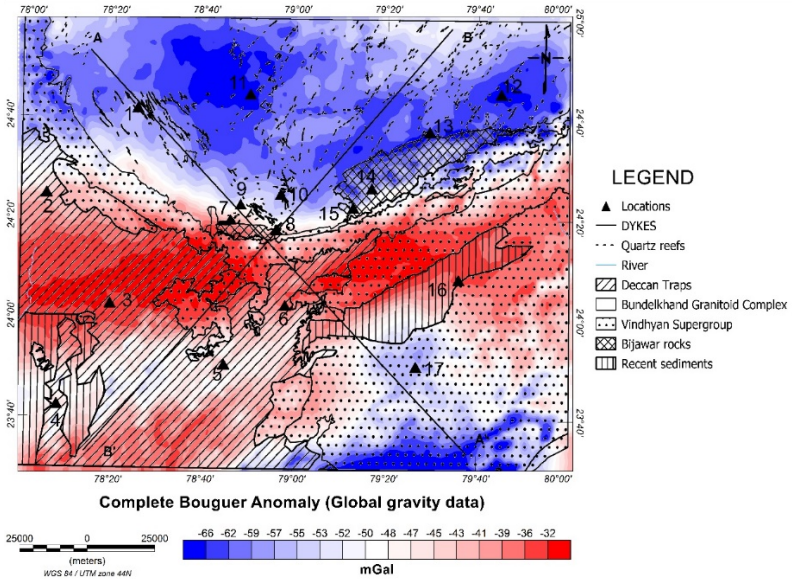

Figure 1: Complete Bouguer anomaly map (lithology map from Figure 1 of manuscript superimposed) obtained using topography and gravity data from global 1-minute topography and free-air gravity grids available on the website of the Scripps Institution of Oceanography, (https://topex.ucsd.edu/WWW_html/mar_topo.html; https://topex.ucsd.edu/cgi-bin/get_data.cgi). Locations: (1)Lalitpur, (2)Mungaoli, (3)Khurai, (4)Gyaraspur, (5)Sagar, (6)Banda, (7)Sonrai, (8)Girar, (9)Madawara, (10)Karitoran, (11)Tikamgarh, (12)Chhatarpur, (13)Bijawar, (14)Dargawan, (15)Hirapur, (16)Hatta, (17)Damoh.

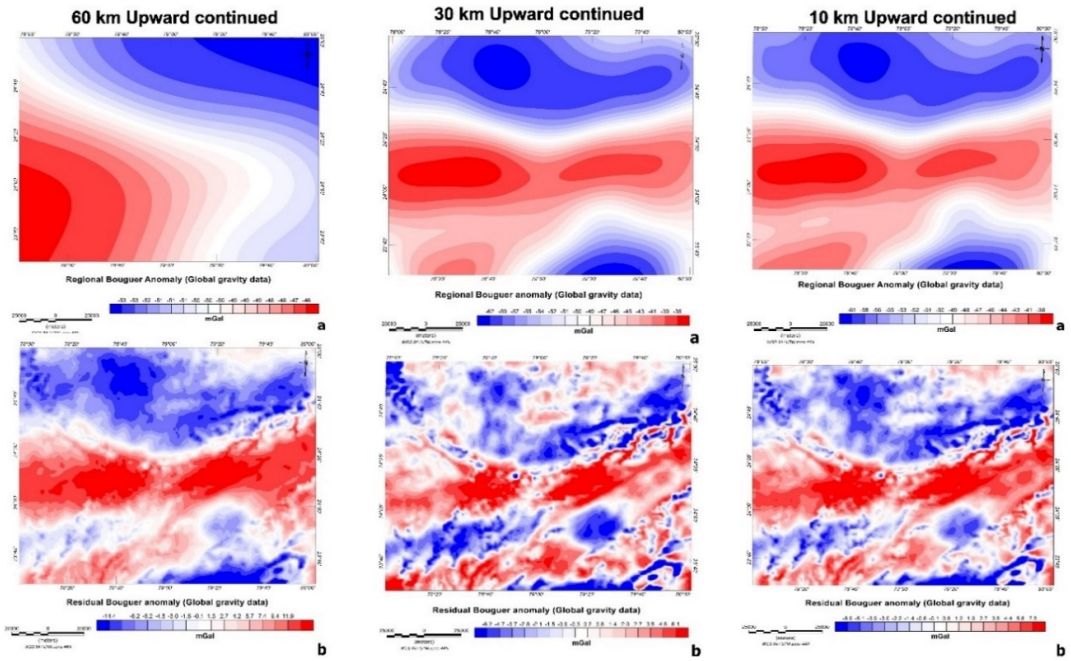

Figure 2: A. (a) Regional gravity anomaly map of the global gravity data, upward continued up to 60 km, (b) Residual gravity anomaly map of the global grid data, obtained after subtracting the 60 km upward continued regional gravity anomaly from complete Bouguer anomaly. B. (a) Regional gravity anomaly map of the global gravity data, upward continued up to 30 km, (b) Residual gravity anomaly map of the global grid data, obtained after subtracting the 30 km upward continued regional gravity anomaly from complete Bouguer anomaly. C. (a) Regional gravity anomaly map of the global gravity data, upward continued up to 10 km, (b) Residual gravity anomaly map of the global grid data, obtained after subtracting the 10 km upward continued regional gravity anomaly from complete Bouguer anomaly.

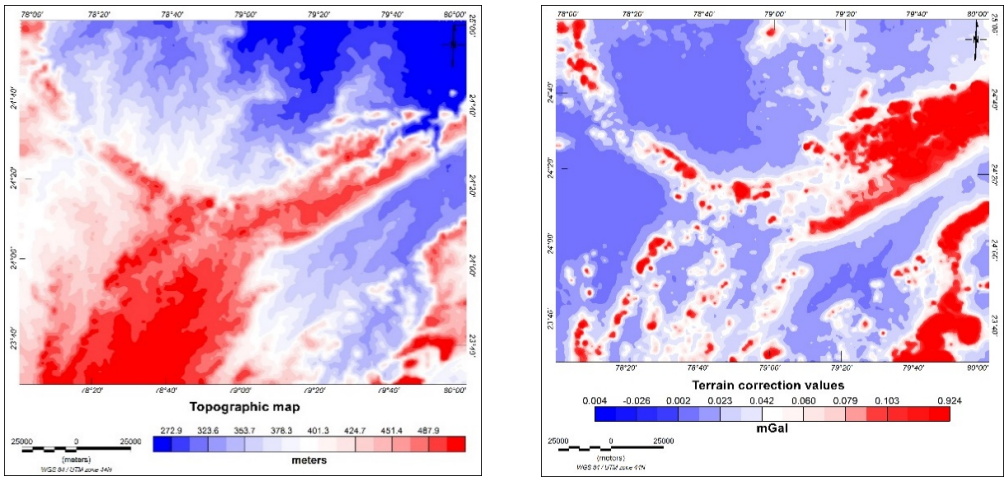

Figure 3: (a) Topographic map derived from the global 1-minute topography grids available on the website of the Scripps Institution of Oceanography, (https://topex.ucsd.edu/WWW_html/mar_topo.html; https://topex.ucsd.edu/cgi-

bin/get_data.cgi), (b) Plot of terrain correction values calculated using the Terrain feature on the Gravity module on Geosoft Oasis Montaj software.

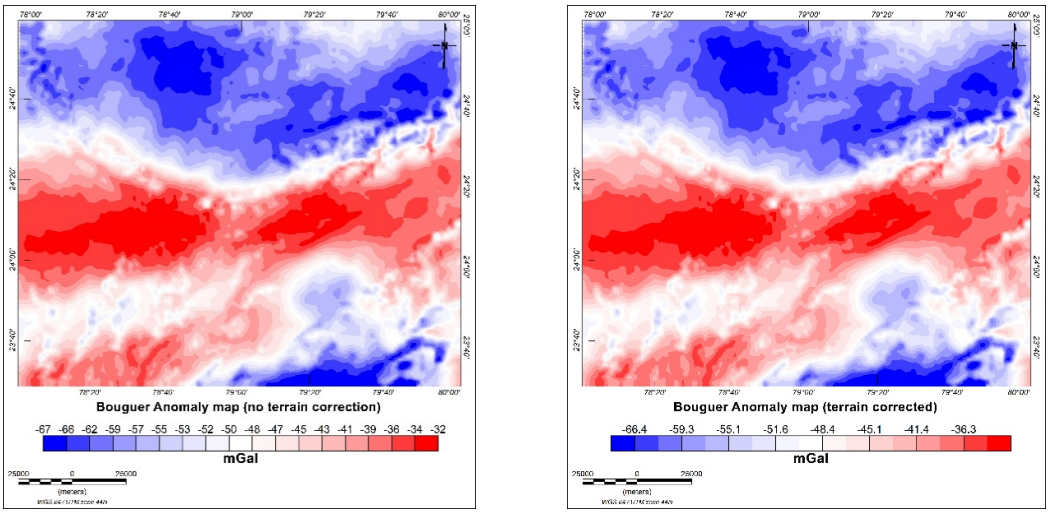

a **b**

Figure 4: (a) Bouguer anomaly map without terrain correction applied, (b) Terrain corrected complete Bouguer anomaly map.

2. *The authors extract the regional Bouguer anomaly trend and separate it from the gravity effect of surface geological structures (residuals). However, they often refer to "Bouguer gravity anomaly" throughout the manuscript.*

   Please, state explicitly which type of gravity data product is used for RAPS analysis, 3D Moho depth inversion, and 2D forward gravity modeling respectively.

   Is the upward-continued regional Bouguer trend used in every analysis? If yes, can it constrain the shallower (hence smaller wavelength) structures in the 2D forward modeling (e.g. basin structures at a few km depth below the surface in Figures 6 and 7)?

   Response: The phrases "observed Bouguer gravity anomaly" and "complete Bouguer anomaly" have been used to describe the gravity anomaly (Fig. 1, see above under the response to comment #1) that is derived based on the application of Bouguer and terrain corrections on the free-air anomaly obtained from the gridded global gravity data. This Bouguer anomaly is used for all the analyses described in the manuscript (i.e., for RAPS, 3D Moho depth inversion, and 2D forward gravity modelling). Maybe the confusion arose due to the phrases "regional Bouguer anomaly" and "residual Bouguer anomaly" being used a few times in the manuscript for describing the resultant regional and residual maps (Figs. 3a and 3b, in the manuscript) from the upward continuation approach.

To avoid further confusion, we have modified the manuscript to denote the terrain corrected Bouguer anomaly as "complete Bouguer anomaly" (Fig. 1, see above under the response to comment #1), while the upward continued regional and calculated residual anomalies as "regional gravity anomaly" and "residual gravity anomaly", respectively.

Once again, we want to clarify here that all the analyses carried out in this study utilize the complete Bouguer anomaly (as given in Fig. 1, see above under the response to comment #1) and this has been mentioned in the Methodology as well as the Results sections. Thus, the shallower structures have been created in the forward models utilizing the complete Bouguer anomaly.

3. *Could the authors spend a few more words on the RAPS technique? The output provides a deep density contrast interface at ca. 30.3 km depth. What is the resolution expected from this technique, which, if I understand well, provides a 1D average information across the study area?*

   Response: The section on radially averaged power spectrum (RAPS) analysis in the manuscript is a concise form of explanation for the technique as this is a well-established and commonly used technique for potential field data interpretation. The detailed mathematical background for the technique can be found in one of the pioneer works in this direction by Spector and Grant (1970). In terms of the resolution of the technique, the reviewer's perspective is valid since the technique estimates the average depth to the top of the assemblage of the source bodies. According to Wahaab et al. (2017), deeper sources can be distinguished from the shallower ones only if they have greater spectrum amplitudes or if the shallower bodies have smaller depth extent. The extent of the depth estimates derived from the RAPS technique depends on the spatial dimension as well as resolution of the data being used. According to Spector and Grant (1970), the depth of exploration for this technique depends on the size of the map being used. Thus, owing to the large latitudinal and longitudinal extent (23.5°–25° N and 78°–80° E) of the study area, we were able to obtain the average depth estimate of ~ 30 km, to deeper interfaces. The global gravity data used here has a spatial resolution of 1-minute, which aids in better examination of the deeper features in the present study area.

4. *The authors perform a 3D inversion for the Moho topography. The algorithm they use requires assuming a mean depth z0 and a density contrast. Why did they use 36 km for z0? And not e.g. 30 km as obtained from the previous RAPS analysis?*

And related to this, how do these results change as a function of z0 and density contrast? Please, provide a sensitivity test for these parameters, and a resolution test for the inversion algorithm application.

Response: We appreciate the suggestions provided by the reviewer here. We did perform the 3D inversion for obtaining the Moho topography using varying values of mean Moho depth (z_0), ranging from 30 km to 38 km (Fig. 5, as given below). The density contrast (i.e., 0.52 g/cm^3) between the mantle and the crust, used for the inversion is obtained by taking the average crustal density value of 2.78 g/cm^3 (all these densities are mentioned in Table 1 of the manuscript as well as the same table has been included below under the response of the comment# 5b). This density contrast was thus kept constant for the varying z_0 values. The inverted Moho topography results obtained using 36 km as the mean Moho depth shows closer correlation with the crustal layer thicknesses and depths suggested in the work by Kumar et al. (2012). The average Moho depth of ~36 km for the Archean crust of the Bundelkhand craton was also presented by Kumar et al. (2012), thus we finalized the results with the assumed z_0 value of 36 km. The variations observed in the obtained inverted Moho topography by varying the mean depth values is presented here in the Figure 5. The results obtained with z_0 values of 30 km, 32 km, and 34 km (Figs 5A, 5B, and 5C, respectively, below), show a very shallow Moho structure below the central region of the study area (ranging from 26 km to 30 km), which is also shallower than the depth estimates to the mafic layer proposed by Kumar et al. (2012). Thus, the results indicate that the estimated Moho depths are changing significantly with 2 km variation in the z_0 values. We also noticed that by varying the density contrast between the mantle and the crust from 0.52 g/cm^3 (including the density of the underplated layer in crustal part) to a density contrast of 0.6 g/cm^3 (without considering any underplating layer in the crustal part), the results (Fig. 6A-B, below) qualitatively remain similar. Thus, the algorithm shows little sensitivity to the change in the assumed density contrast.

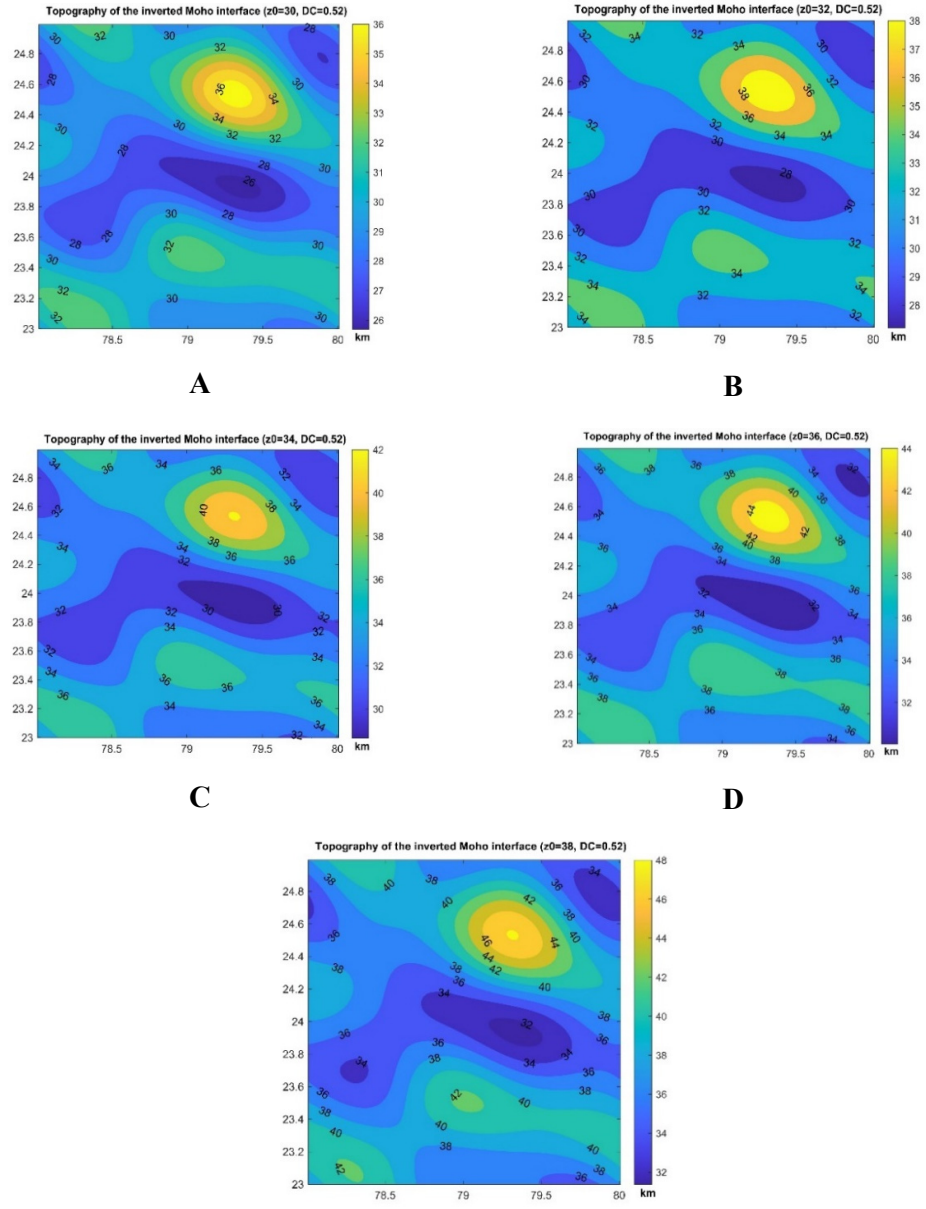

Figure 5: Moho topography map obtained by applying the Parker-Oldenburg method on the complete Bouguer anomaly data of Fig. 1, using 0.52 g/cm^3 as the density contrast, with A. z_0= 30 km, B. z_0= 32 km, C. z_0= 34 km, D. z_0= 36 km, and E. z_0= 38 km.

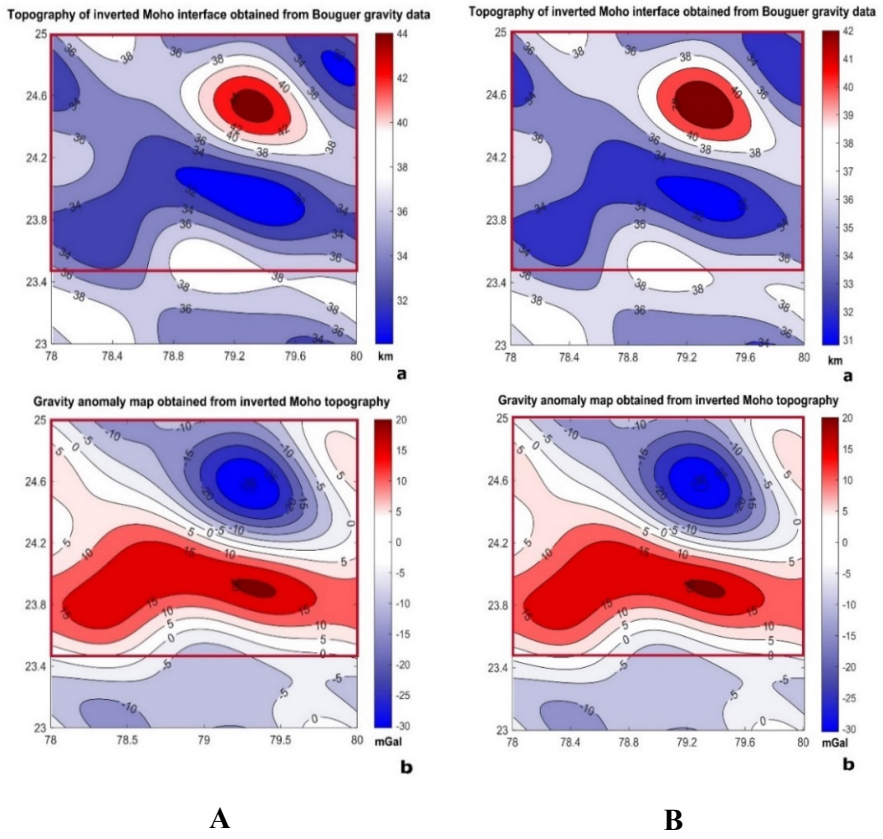

A **B**

Figure 6: A. (a) Moho topography map obtained by applying the Parker-Oldenburg method on the complete Bouguer gravity data of Fig. 1, using 0.52 g/cm^3 as the density contrast. (b) Gravity map obtained using the inverted Moho depths from Fig. 6A(a). The red box marks the study area. B. (a) Moho topography map obtained by applying the Parker-Oldenburg method on the complete Bouguer gravity data of Fig. 1, using 0.6 g/cm^3 as the density contrast. (b) Gravity map obtained using the inverted Moho depths from Fig. 6B(a). The red box marks the study area.

5. *I believe a few important points should be clarified in the 2D modeling stage.*
   The authors perform 2D forward modeling based on the formulas by Talwani et al. (1959). These formulas are best suited when both the data, and the target area, present a 2.5D symmetry (e.g. changing properties along the x-z plane, and no changes along y-axis); see e.g. Scarponi et al. (2021), Frontiers for one example. In particular, profile AA' seems not to be perpendicular to visible 2.5D structures, nor in the gravity data or in the underlying, inverted Moho structure (based on Figure 2 and Figure 5a). A slight-to-moderate rotation of profile AA' around its center (e.g. +20 degrees) could potentially provide a different gravity data profile, and hence lead to different results and interpretation.
   a) *The authors could consider using a 3D inversion software (see e.g. IGMAS+ in Spooner et al. 2019, Solid Earth). If not 3D, how would the 2D gravity profiles (data and models) look like along a set of parallel profiles (e.g. at constant longitude)? Would the results,*

and hence interpretation, change along a different profile than AA'? This should be tested and discussed before interpretation.

b) *Paragraph 3.5 on the construction of the 2D profiles never mentions incorporating the results from the 3D Moho depth inversion. Were these Moho results neglected in the creation of the 2D models shown in Figure 6 and 7? If yes, why?*

   The authors mention the RAPS estimate as reference used in the profiles, but RAPS provides an inherently 1D average information. Moreover, profile BB' shows no interfaces around 30 km: please, can the authors explain the reason for this?

   According to Figure 5a, the computed Moho depths obtained along BB' range from 44 km to 34 km depth, but this seems not to be the case when looking at Figure 7. This should be clarified (partially applies also to profile AA' and Figure 6).

c) *In the definition of the structures within profiles AA' and BB', the authors refer to a list of previous investigations, to be used as external constraints. This is OK in principle. However, these external constraints are not explicitly indicated in Figure 6 and 7.*

   Which geometries were imported as unmodified external information? Which ones were generated and/or modified by the authors? This information is not clear and should be made explicit. The authors could also show in Figures 6 and 7, how their new Moho estimate compares to the external information they refer to.

   Clarifying the points above is important to discuss the fit to the gravity data along the selected profiles. For example, was the geometry of the underplating structure in Figure 7 imported from external sources? How would the forward modeling compare to the data, with a different, or without, the underplating layer along AA'?

To address these points, I would advise starting by: 1) apply RAPS; 2) use the RAPS deepest interface estimate as z0 for the Moho inversion (provide sensitivity and resolution tests); 3) use the obtained Moho depth as starting geometrical constraint, together with those existing in the literature, either for 3D modeling, or for a set of 2D profiles (as much as possible along structures with 2.5D symmetry), providing support for the chosen 2D profiles; 4) test if the deeper underplating layers can be resolved by gravity along the chosen profiles.

Response: We want to clarify here that we have utilised the GM-SYS profile module of the Oasis Montaj software for performing the 2D forward modelling along the two profiles. As per the GM-SYS User's Guide, the 2D forward modelling responses are based on the methods of Talwani et al. (1959), and Talwani and Heirtzler (1964), that make use of the algorithms given by Won and Bevis (19870). It also performs 2.5D calculations based on the method of Rasmussen and Pedersen (1979). These methods and algorithms are combined to improvise the

efficiency of the features of GM-SYS profile module to enable 2¾-D forward modelling (Oasis Montaj GM-SYS manual). Thus, this module helps in developing 2-D forward models, 2¾-D forward models as well as skewed models where the strike direction may not be perpendicular to the profile. The E-W trending (approximately) gravity high in the central region of Figure 1, presented here, is not exactly perpendicular to the two profiles but they intersect the anomaly feature (also the inferred underplated layer) at an angle. Since the GM-SYS profile can be utilized to develop models along such profiles, the chosen profiles were eventually used.

a) We appreciate suggestions provided here by the reviewer. Previously, models were developed along profiles at constant longitudes, but the individual profiles did not span all the lithological units of interest to give a better understanding of the crustal structure below the study area. Hence, the present profiles were utilized for the forward models. The methodology utilized here are chosen to provide validation to the plume/superplume hypothesis suggested by Mishra (2015) by showing the presence of the underplated layer at lower crustal depths. The trend of the Moho structure (as obtained from forward model) and the depth variations observed from the inverted Moho topography show some correlation with the layering information from Kumar et al. (2012). This can be also observed in the Distance vs. Moho depth plot using the inverted Moho topography (as obtained from Parker-Oldenburg inversion method) along with the Moho depth with and without the thickness of underplated layers as obtained from forward models along the profiles AA' and BB' (Figs. 7a and 7b, below). These plots show that the general trend of the underplating interface from the forward model and the trend of the Moho structure from the inversion results show similarity along the profiles AA' (Fig. 7a) and BB' (Fig. 7b). However, the inversion scheme is unable to distinguish the underplated layer from the Moho depth level unlike the forward modeling scheme. Therefore, the forward models represent more refined and better-constrained results which follow the broad trend of inversion results.

   We are also grateful to the reviewer for their suggestion of the IGMAS+ software and we will attempt to accommodate results from it in future work.

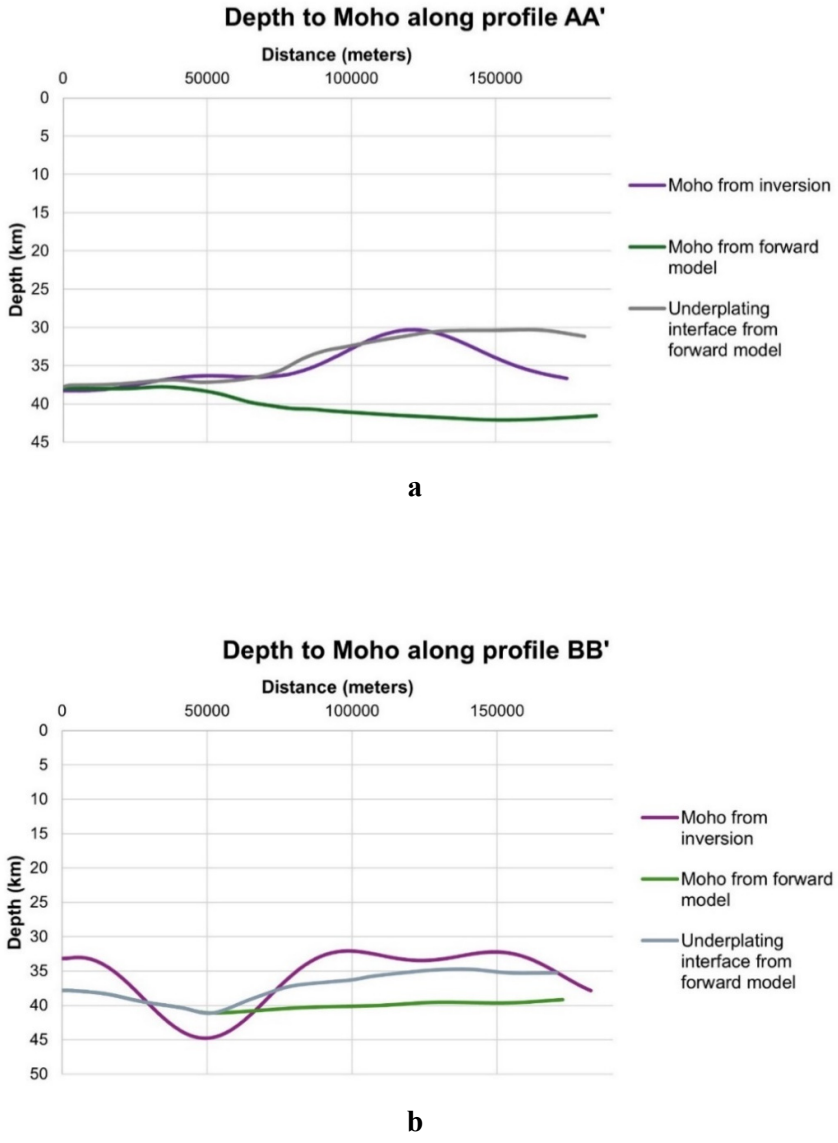

Figure 7: (a) Distance vs. Moho depth plot using the inverted Moho topography, Moho interface from the forward model, and underplating interface from the forward model along the profile AA'. (b) Distance vs. Moho depth plot using the inverted Moho topography, Moho interface from the forward model, and underplating interface from the forward model along the profile BB'

b) We acknowledge the observation made by the reviewer here. However, we want to clarify that the depths used in the gravity modeling are a combination of the results obtained from RAPS analysis, inverted Moho topography, and the crustal layer thicknesses obtained from prior literature. The average depth estimates of 30 km to the deepest interface as per the RAPS analysis helped in constraining the depth to the top

of the underplated layer. The depth to top of the underplated layer corresponds to the region showing shallowest Moho depths in the inverted Moho topography results, which corroborates with the findings of Kumar et al. (2012) and hence is used as a constraint too. The difference in the Moho depths for the regions in the forward models and the inverted Moho topography below the Bundelkhand craton is possibly observed as the forward models have been constructed by adjusting the layer thicknesses, and depths according to the above-mentioned constraints. Also, the density contrast (0.52 g/cm^3, with the density of the underplated layer, Fig. 6A) used for the inversion may not apply objectively for the region below Bundelkhand craton since it is most absent below the craton. As briefly discussed in the response to comment #4 above, we performed the Moho depth inversion with the density contrast (between Mantle and crust) values of 0.52 g/cm^3 (using the average crustal density including the underplating density, Fig. 6A) and 0.6 g/cm^3 (using the average crustal density eliminating the underplating density, Fig. 6B). The results (Figs. 6A,6B) follow similar trends as the results shown in the manuscript, and the Moho values below the Bundelkhand craton and in the central region (below the Vindhyan rocks) show similar ranges of values. Thus, we observed that the inversion results are unable to distinguish the density contrast due to the underplated layer. The Moho depth ranges for regions covered by the Bundelkhand craton and the Vindhyan basin as suggested by Kumar et al. (2012) have been used as a constraint for the region of the modelled underplated layer, which varies from ~36 km to ~44 km. These depth ranges were used as constraints with a trial-and-error approach for the forward modelling while keeping the density values consistent with the density contrast utilized for the inversion method. Thus, the forward models represent more refined and better-constrained results which follow the broad trend of inversion results.

c) Due to the non-availability of sufficient studies over the present study area, along the southern margin of Bundelkhand craton, the gravity modelling is constrained with only limited information. Few of the existing geophysical studies (Kumar et al., 2012; Gokarn et al., 2013; Mishra, 2015) on the Bundelkhand craton have suggested plume/superplume setting one of the formation mechanisms of the Proterozoic basins of this region and even proposed the presence of an underplated mafic layer below the basins. There is a lack of a detailed subsurface model delineating the spatial and depth extent of the underplated layer based on geophysical observation and its correlation

with the formation of the Proterozoic basins along the southern margin of the Bundelkhand craton and adjoining areas. For the forward modelling here, the thicknesses for the different layers are majorly constrained by the results from the wide-angle seismic study along the Hirapur-Mandla profile by Sain et al. (2000) and the shear velocity structure obtained by Kumar et al. (2012). Best attempts have been made to carefully stick to the prior established density values as mentioned in Table 1. The density and thickness of the underplated layer are modified and adjusted by a trial-and-error approach to fit the gravity response curve, keeping the error between the calculated and observed gravity response as low as possible. The Moho depth for the Sagar station (~44km) suggested by Kumar et al. (2012) has been used as a constraint for the region where the underplated layer is modelled but cannot be displayed on the forward model since it is not directly lying on the BB' profile. The geometry of layers forming the basin structure is modified using the information and models provided by Basu and Bickford (2015), Mishra (2015). The structure of the underplated is essentially adjusted by the previously addressed trial-and-error approach, with inputs from Kumar et al. (2012) as well as the Moho inversion results. As discussed in the response to comment #5a, it is observed in Figure 7 that the general trend of the top surface of the underplated layer from the forward model and the trend of the Moho structure from the inversion results show similarity beneath the profiles AA' (Fig. 7a) and BB' (Fig. 7b). All these details related to the past tectonic evolution information and the constraints used for gravity modelling are discussed in the sections '2 Geological background' and '3.5 Two-dimension forward gravity modelling', respectively.

Table 1: Density values used in the present study, compiled from established literature.

Layers	Density (g/cm^3)	References
Recent sediments	2.1	Prasad et al. (2018)
Vindhyan supergroup	2.5	Mishra (2015); Pal and Kumar (2019)
Bijawar basement of Vindhyan	2.84	Mishra (2015
Bundelkhand granite + basement, Upper crust (average)	2.64	Podugu et al. (2017); Pati and Singh (2020)
Deccan traps	2.85	Rao et al. (2011)
Average Middle and Lower crustal density	2.8	Rao et al. (2011); Chouhan et al. (2020)

We highly appreciate the suggestions provided by the reviewer on the tentative steps to be carried out. We would like to clarify that the workflow of our chosen methodology follow a similar approach as suggested by the reviewer here, and consequently have presented the results from RAPS analysis, inversion, and forward modelling. We have incorporated all the suggestions put forth by the reviewer to justify our findings as well as refine the existing manuscript for publication.

Response to additional comments:

- *Figure 1b is not readable and should be larger. Figure 1a is readable, but please consider using different colors to highlight the different geological units. The perimeter box of figure 1a should appear in figure 1b to show its location;*

  Response: We apologize if the Figure 1 (of the manuscript) caused a confusion between Figure 1a and Figure 1b (of the manuscript). We have modified the Figure 1 of the manuscript (here given below as Fig. 8) and the location of the study area is now shown in Figure 8a as a red box. The pattern scheme has been utilized for highlighting the geological units so that this figure can be superimposed with ease on the anomaly maps.

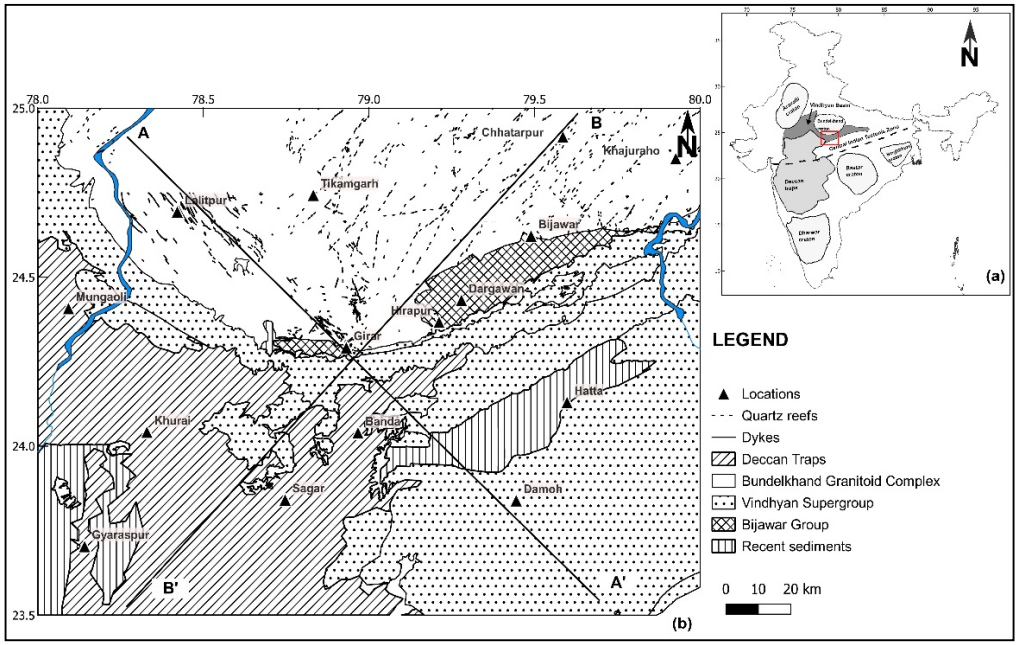

Figure 8: (a) Position of the Bundelkhand craton and Vindhyan basin with respect to other major cratons of the Indian subcontinent. Bijawar basin forms the base of the Vindhyan basin and the exposed sequences are shown in Figure 1b. (b) General geological setup of the region used for the regional scale study of the craton and surrounding areas along the southern boundary of the craton. The two profiles used for gravity modelling are marked here as AA′ and BB′.

- *Figure 5 should at least contain a residual map (synthetics minus observations).*
  It would be also beneficial to add a plot for RMS versus iteration number, to show the RMS reduction during the inversion, and a sensitivity and resolution tests (possibly in a different Figure)

  Response: We hope here, by residual the reviewer is indicating the difference between the observed gravity anomaly and the calculated gravity from the inverted Moho topography and the same has be given in Figure 9 (below). The convergence criterion of 0.02 is reached by the 3rd iteration with the RMS error value of 0.012106, while performing the inversion with z_0 value of 36 km and density contrast of 0.52 g/cm^3.

  The Parker-Oldenburg algorithm-based Moho depth inversion scheme was introduced by Gomez-Oritz and Agarwal (2005), and it is a well-established approach. Detailed resolution and sensitivity tests are not performed here, like some of the works using this approach done by previous authors (e.g., van der Meijde et al., 2013; Windhari and Handayani, 2015; Bessoni et al., 2020; Ydri et al., 2020). However, as per the reviewer's comments we examined the sensitivity of the inversion scheme with respect to the varying mean depth z_0 and density contrast as discussed in the response for the comment #4 above.

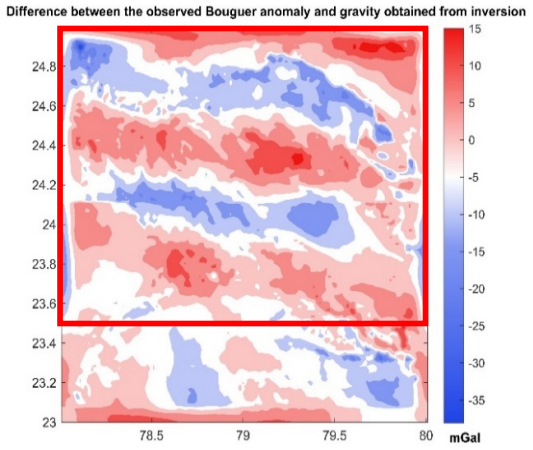

Figure 9: Difference in Gravity between the observed complete Bouguer anomaly map (Fig. 1, above under the response for comment #1)) and that obtained using the inverted Moho topography derived from Parker-Oldenburg algorithm, for z_0=36 km and density contrast of 0.52 g/cm^3. The red box marks the study area as seen in the adjacent regional anomaly map.

- *Figure 6 and 7 should show explicitly which geometries were imported as unmodified external constraints for the construction of the models. They should also show the Moho depth as obtained from the 3D inversion (Figure 5a).*

  Response: We have clarified the same concern raised by the reviewer in the comment #5c above. To show the trends followed by the Moho structure in the forward models as well

as the inversion results, we have provided the plots of Distance vs Depth to Moho along the profiles AA' and BB' (Figs. 7a and 7b, respectively above).

- *Also, the top banner in Figures 6 and 7 is not very clear: is it gravity or Bouguer anomaly? Please, plot the error on a separate independent scale to be more readable.*
  Response: These modifications have been made in the modified manuscript figures.

- *line 175: by "Bouguer anomaly" you mean the upward-continued regional trend? Please, specify. Same for line 219, 239, 270, 286, 295 and so on.*
  Response: We have clarified the similar concern raised by the reviewer in the comment #2 above. Bouguer anomaly always refer to the gravity anomaly caused by the subsurface anomalous masses/structures and include the response of both shallower and deeper features. On the other hand, the upward-continued regional trend represent the response due to deeper features i.e., regional component of Bouguer anomaly. Therefore, Bouguer anomaly and the upward-continued regional map are different. To avoid any confusion (if there), we have modified the manuscript to denote the terrain corrected Bouguer anomaly as "complete Bouguer anomaly" (Fig. 1, see above under the response to comment #1), while the upward continued regional and calculated residual anomalies as "regional gravity anomaly" and "residual gravity anomaly", respectively.

- *Line 244: Does GMSYS perform 2D forward modeling or 2D inversion?*
  This is a crucial detail. If it performs inversion, then more information is needed here. Or, have you tested several candidate profiles? Please, explain.
  Response: The GM-SYS profile module is only used for 2D forward modelling in this study here, however this module is capable of inversion too, which has not been used here.

- *Line 375-377: To my understanding, you obtain a Moho from 3D gravity inversion. But you do NOT obtain a Moho depth from 2D forward gravity modeling (see also question above). If you do not perform 2D inversion, then 2D forward modeling can only validate a certain profile, but not "provide" or "obtain" from it. This is better formulated later in the conclusions, at line 442 "[...] validated by the 2D [...]". Please, This should be clarified. And finally, why not using the 3D Moho results in the construction of the 2D models?*
  Response: We are thankful to the reviewer for raising this concern, and the concerned statements has been modified, since the forward models validate the presence of the

underplated layer, and the Moho structure as suggested by Kumar et al. (2012). We have already clarified part of this query in the response to the comment #5b regarding the use of Moho inversion results in the development of the forward models.

REFERENCES

Basu, A. and Bickford, M. E. An alternate perspective on the opening and closing of the intracratonic Purana basins in peninsular India, Journal of Geological Society of India 85(1), 5–25, 2015.

Bessoni, T. P., Bassrei, A., and de Oliveira, L. G. S.: Inversion of satellite gravimetric data from Recôncavo-Tucano-Jatobá Basin System, Brazilian Journal of Geology 50(3), 1–14, 2020.

Gao, X. and Sun, S.: Comment on "3DINVER.M: A MATLAB program to invert the gravity anomaly over a 3D horizontal density interface by Parker-Oldenburg's algorithm", Computers & Geosciences 127, 133–137, 2019.

Gómez-Ortiz, D. and Agarwal, B. N. P.: 3DINVER.M: A MATLAB program to invert the gravity anomaly over a 3D horizontal density interface by Parker-Oldenburg's algorithm. Computers and Geosciences, 31(4), 513–520, 2005.

Gupta, V. K., and Ramani, N. Some aspects of regional-residual separation of gravity anomalies in a Precambrian terrain. Geophysics 45: 1412-1426, 1980.

Jacobsen, B.H. Case for upward continuation as a standard separation filter for potential-field potential-field maps. Geophysics 52, 1138–1148, 1987.

Kebede, H., Alemu, A., Fisseha, S. Upward continuation and polynomial trend analysis as a gravity data decomposition, case study at Ziway-Shala basin, central Main Ethiopian rift. Heliyon, 6, 2020.

Kumar, T. V., Jagadeesh, S., and Rai, S.S.: Crustal structure beneath the Archean–Proterozoic terrain of north India from receiver function modelling, Journal of Asian Earth Sciences 58, 108–118, 2012.

Meng, X., Guo, L., Chen, Z. Shuling, L., and Lei, Shi. A method for gravity anomaly separation based on preferential continuation and its application. Appl. Geophys. 6, 217–225 2009.

Mishra, D. C.: Plume and Plate Tectonics Model for Formation of some Proterozoic Basins of India along Contemporary Mobile Belts: Mahakoshal — Bijawar, Vindhyan and Cuddapah Basins, Journal of the Geological Society of India 85(5), 525–536, 2015.

Oasis Montaj GMSYS manual: http://updates.geosoft.com/ downloads/Bles/how-to-guides/GM-SYS˙ProBle˙Create˙ New˙Model.pdf.

Pal, S. K. and Kumar, S.: Subsurface Structural Mapping using EIGEN6C4 Data over Bundelkhand Craton and Surroundings: An Appraisal on Kimberlite/lamproite Emplacement. Journal of the Geological Society of India, 94(2), 188–196, 2019.

Rasmussen, R., and Pedersen, L. B.: End corrections in potential field modeling: Geophysical Prospecting, 27, 749-760, 1979.

Sain, K., Bruguier, N., Murty, A. S. N., and Reddy, P. R.: Shallow velocity structure along the Hirapur-Mandla profile using travel time inversion of wide-angle seismic data, and its tectonic implications. Geophysical Journal International 142(2), 505–515, 2000.

Smith, W. H. F., and Sandwell, v D. T.: Global seafloor topography from satellite altimetry and ship depth soundings, Science, v. 277, p. 1957-1962, 26, 1997.

Spector, A. and Grant, F. S.: Statistical methods for interpreting aeromagnetic data, Geophysics 35, 293–302, doi:10.1190/1.1440092, 1970.

Talwani, M., Worzel, J. L., and Landisman, M.: Rapid gravity computations for two-dimensional bodies with application to the Mendocino submarine fracture zone: J. Geophys. Res., 64, 49-59, 1959.

Talwani, M., and Heirtzler, J. R.: Computation of magnetic anomalies caused by two-dimensional bodies of arbitrary shape, in Parks, G. A., Ed., Computers in the mineral industries, Part 1: Stanford Univ. Publ., Geological Sciences, 9, 464-480, 1964.

Van der Meijde, M., Julià, J., and Assumpção, M.: Gravity derived Moho for South America. Tectonophysics 609, 456–467, 2013.

Wahaab, F. A, Lawal, S. K., Adebayo, L. L.: Spectral Analysis of Higher Resolution Aeromagnetic Data over Some Part of Kwara State, Nigeria., International Journal of Engineering Research & Technology (IJERT) Volume 06, Issue 03, 2017.

Windhari, A. and Handayani, G.: Gravity data inversion to determine 3D topographical density contrast of Banten area, Indonesia based on fast Fourier transform, In AIP Conference Proceedings (Vol. 1656), American Institute of Physics Inc., 2015.

Won, I. J., and Bevis, M.: Computing the gravitational and magnetic anomalies due to a polygon: Algorithms and Fortran subroutines: Geophysics, 52, 232-238, 1987.

Ydri, A., Idres, M., Ouyed, M., and Samai, S.: Moho geometry beneath northern Algeria from gravity data inversion, Journal of African Earth Sciences, 168, 2020.